Heliyon 9 (2023) e17015

Contents lists available at ScienceDirect

Heliyon

journal homepage: www.cell.com/heliyon

Differences in symmetrical low-frequency oscillations among healthy subjects, and those with stroke or peripheral arterial disease

Yunfei Ma [a], Kexin Luo [a], Peng Ding [a], Shimin Yin [b], Xiaoli Li [c,**], Yingwei Li [a,*]

[a] School of Information Science and Engineering, Yanshan University, Qinhuangdao, Hebei, 066004, China
[b] Department of Neurology, PLA Rocket Force Characteristic Medical Center, Beijing, 100088, China
[c] Center for Collaboration and Innovation in Brain and Learning Sciences, Beijing Normal University, Beijing, 100875, China

ARTICLE INFO

Keywords:
Systemic low-frequency oscillations
Ischemic stroke
Peripheral atherosclerosis
Symmetrical

ABSTRACT

Objective: Low-frequency oscillations (LFOs) observed in near-infrared spectroscopy (NIRS) reflect autonomic physiological processes, and may serve as useful indicators for detecting and monitoring circulatory dysfunction. The aim of this study was to reveal whether LFOs can be used as vascular perfusion biomarkers to differentiate different types and degrees of vascular lesions based on clinical patient data. *Materials and Methods*: In this study, healthy controls, ischemic stroke patients and peripheral atherosclerosis patients completed a resting-state LFO detection experiment. LFOs were collected simultaneously at peripheral right and left earlobes, fingertips and toes, along with coherence and phase shift analyses processing. *Results:* The results showed that the coherence coefficients of symmetric peripheral positions and the absolute value-phase shifts of fingers and toes can be used to distinguish healthy individuals, ischemic stroke patients and peripheral atherosclerosis patients. The symmetric earlobes' absolute value-phase shifts could be used to differentiate mild and severe ischemic stroke patients; the coherence coefficients and absolute value-phase shifts of the symmetric toes could be used to differentiate mild and severe peripheral arteriosclerosis patients. The accuracy of differentiating between types of patients was 70%; those with different degrees of peripheral atherosclerosis was 85%, and those with different degrees of ischemic stroke was 72%. *Conclusions:* LFOs can serve as vascular perfusion biomarkers to differentiate types and degrees of vascular lesions. Therefore, LFOs have the potential to provide valuable patient information to assist researchers and clinicians in identifying specific peripheral circulatory damage subgroups.

1. Introduction

Low-frequency oscillations (LFOs) in the range of 0.01–0.15 Hz, are normally observed in functional imaging studies, such as blood oxygen level-dependent functional magnetic resonance imaging (BOLD fMRI) [1] and functional near-infrared spectroscopy (fNIRS) [2]. They have been found to travel with the blood flow to different parts of the body [3], and may have value in indicating the presence of abnormal blood circulation. However, no studies have been conducted to validate this hypothesis in clinical patients with

* Corresponding author.
** Corresponding author.
E-mail addresses: xiaoli@bnu.edu.cn (X. Li), lyw@ysu.edu.cn (Y. Li).

https://doi.org/10.1016/j.heliyon.2023.e17015
Received 6 March 2023; Received in revised form 30 May 2023; Accepted 4 June 2023
Available online 5 June 2023

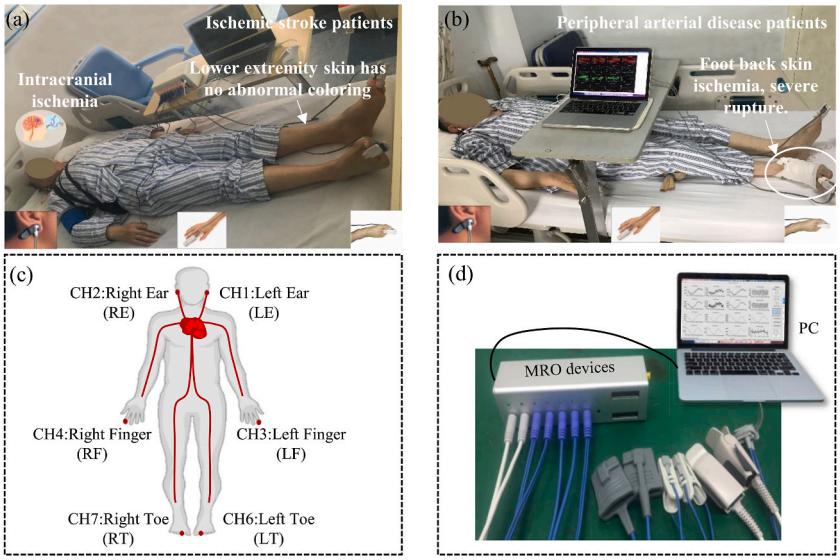

Fig. 1. LFO detection experiment for (a) ischemic stroke patients and (b) peripheral arterial disease patients, (c) specific LFO position detection and (d) MRO system for LFO detection.

different types of vascular injuries. There have also been no studies to provide LFO-based parameters that can be used to distinguish between these types. This is not conducive to the further development and application of LFOs.

In several pioneering studies, LFOs has been observed in infants [4] and adults [5]. The origins of these oscillations remain unclear, and the terminology to describe them is confusing (e.g., spontaneous oscillations [6], low-frequency waves or oscillations [7]). They are often interpreted as indications of the activity of related neurons in different parts of the brain. Some of these LFOs are nonneuronal and reflect autonomic physiological processes. Most studies define the center frequency to be around 0.1 Hz [8], but the range of frequencies varies, with a common range being 0.04–0.15 Hz [9].

Initially, most scholars focused on LFOs in the brain and ignored the periphery. In 2012, a concurrent NIRS and fMRI study revealed a strong correlation between the LFOs measured in the periphery (NIRS signals) and those in the brain (BOLD fMRI) with varying time delays [10]. These findings are the first to indicate the potential value of peripheral LFOs in the study of systemic blood circulation. However, only three peripheral positions (left and right toes and left finger) were detected in their study. The signal detection positions were not comprehensive. Subsequent studies [11] have included improvement of the signal detection position, which was set as left and right earlobes, left and right fingers and left and right toes, and three experimental states have been explored: resting state, paced breathing and passive leg raising. The results show that the symmetrical transmission of LFOs in healthy subjects at resting state indicates that these signals may originate from the heart/lung system. These signals can travel with the blood throughout the body, suggesting that these signals may be able to serve as biomarkers for evaluating vascular integrity. However, these studies have only focused on healthy subjects; there have been no studies of patients with vascular injury to verify LFOs' effectiveness in assessing vascular injury disease. Further, a study [12] was conducted to detect LFOs in stroke patients, and it was found that embolization broke the symmetry of LFO transmission. This confirmed that LFOs could be used as biomarkers for vascular perfusion to distinguish healthy subjects from stroke patients. However, this study did not indicate whether LFOs could distinguish patients with different types and degrees of vascular injuries. In addition, in the aforementioned studies, feature extraction and analysis only focused on time domain correlation and delay estimation, but ignored frequency domain.

Given the above state of the research and existing problems, the contributions of the present study are: 1) We investigated the frequency domain characteristic differences among LFOs in three subgroups: ischemic stroke, peripheral atherosclerosis patients and healthy controls, and in two degrees: mild and severe ischemic stroke, mild and severe peripheral atherosclerosis patients, confirming that LFOs as hemodynamic parameter variations can be used to distinguish types and degrees of vascular injuries. 2) We clarified the classification boundary between types and degrees of patient subgroups, and provided reference standards for further research and clinical application of LFOs.

2. Materials and methods

2.1. Participants

We prospectively recruited 25 ischemic stroke patients (7 F, 18 M, age = 70.1 ± 11.4 y.o.; mean ± SD, range = 44 to 90 y.o.) and 14 peripheral atherosclerosis patients (6F, 8 M, age = 74.2 ± 12.9 y.o.; mean ± SD, range = 51 to 87 y.o.) from Rocket Force Characteristic Medical Center. We also recruited 25 healthy subjects (12F, 13 M, age = 35.5 ± 10.0 y.o.; mean ± SD, range = 21 to 59 y.o.) as controls. The Institutional Review Board at McLean Hospital and Rocket Force Characteristic Medical Center approved the protocol.

Experienced clinicians and their teams were invited to discuss the clinical diagnosis results of all patients in this study. Less than 60% vascular stenoses was considered mild to moderate, while greater than 60% was considered severe. After adjusting for National Institute of Health stroke scale (NIHSS) and limb muscle strength, 14 and 11 patients with mild and severe ischemic stroke, and 8 and 6 patients with mild and severe peripheral atherosclerotic disease were categorized, respectively.

2.2. Procedure

Each experiment began with an explanation of the procedure to each participant or their guardian, and then giving them informed consent. We cleaned each participant's left earlobe (LE), right earlobe (RE), left index fingertip (LF), right index fingertip (RF), left index toe (LT) and right index toe (RT) with alcohol swabs to ensure a stable connection, and placed six pulse oximeter probes at the peripheral measurement positions, as shown in Fig. 1(a) and (b). The specific signal acquisition positions are shown in Fig. 1(c). In the processes of LFO acquisition, the patient's movements may produce motion artifacts, resulting in the uncertainties signals. Under normal circumstances, the experiment would last about 12 min, and we would delete any unstable data at either end of the data segment to increase overall stability, and retain 10 min of data from six peripheral positions. The participants were in a supine position on a comfortable bed with their eyes open, in a room with dim light, an indoor temperature of 25 °C, relative humidity of 30%–40%, and air pressure of 100k Pa. They were instructed to relax and breathe evenly, and asked to remain still in a resting state (RS) during the experiments.

Typically, pulse oximeters measure only a single channel and remove low frequency signals with a high-pass filter to focus on the cardiac waveform. To record LFOs at multiple peripheral positions, we had to develop our own multichannel NIRS oximeter [multichannel research oximeter (MRO)] based on standard photoplethysmograph hardware with modified acquisition software [13]. The MRO sampling frequency was 31.25 Hz, which was sufficient to sample LFOs (0.01 Hz–0.15 Hz) without aliasing. The device is shown in Fig. 1(d).

2.3. LFO processing and analysis

According to the modified Beer-Lambert law, we transformed data measured by two wavelength (660 nm and 920 nm) light sources into the concentration changes of oxygenated hemoglobin (Δ[HbO]) and deoxygenated hemoglobin (Δ[HbR]), respectively [14]. In several existing studies, optical path difference factor (DPF) values approximating tissue thickness have been calculated through Monte Carlo simulation and human experimental data. Therefore, we used DPF values slightly greater than the mean thickness of the earlobes, fingertips and toes in this study [15]. We performed further data processing and analysis with MATLAB (The MathWorks, Inc.). Through the zero-phase Butterworth band-pass filter (MATLAB function of filtfilt.m, butterworth order = 3), we extracted the low-frequency oscillations in the frequency range of 0.01 Hz–0.15 Hz [11]. Two methods were applied to reduce the impact of motion artifacts: (1) we used cubic-spline interpolation [16] to remove the motion artifacts of unexpected sudden movements (e.g., sweeping gestures and sudden head movements); (2) we used kurtosis-based wavelet filter [17] to remove the motion artifacts of spontaneous quivers (i.e., stroke patients' neurological disorders due to vascular thrombosis). To increase the sample set's fault tolerance, we processed the data through a moving window, and divided 600 s data into 11 subsets. All 11 subsets were included in the analysis, and this allowed us to assess the phase shifts' stability and calculate the coherence over the entire data set.

The coherence is an extension of the Pearson's correlation coefficient. The difference from the correlation is that the coherence is time-locked, and used to evaluate the spectral cross-correlation of the normalized power spectra [18]. The coherence coefficients can reflect the frequency domain similarity of LFOs in different parts. The coherence coefficients are calculated as follows [19][]:

$$R_{xy}(f) = \frac{\left|P_{xy}(f)\right|^2}{|P_{xx}(f)| \cdot \left|P_{yy}(f)\right|}^{[19]} \tag{1}$$

where $P_{xy}(f)$ represents the mutual power spectrum of two signals, while $P_{xx}(f)$ and $P_{yy}(f)$ respectively represent the self-power spectrum of signal x and y.

It has been suggested that the phase of oxygenation and deoxygenation is the key to understanding hemodynamic mechanisms and brain function [20]. Taga et al. [21] have used oxygenation and deoxygenation and its phase-locking index to spatially evaluate brain development in infants. These studies suggest that the phase difference is an important biomarker for analyzing the hemodynamic characteristics. The phase difference between singals x and y can be expressed as:

$$\Delta\varphi(t) = \varphi_x(t) - \varphi_y(t)^{[21]} \tag{2}$$

where $\varphi_x(t)$ and $\varphi_y(t)$ represent the real-time phase of vectors x and y respectively.

We used a rank-sum test to extract the significant differences. In order to reduce the error rate in the positive results, we used the Benjamini-Hochberg method to correct the results [12]. Finally, we used discriminant analysis (the MATLAB function classify.m) to establish classified boundary equations between patients with different types and degrees. The focus of this study's analysis was oxy-hemoglobin (Δ[HbO]), which has a higher signal-to-noise ratio (SNR) than deoxy-hemoglobin (Δ[Hb]) [22,23]. However, it is also possible that the veins (which contain more Δ[Hb]) are less reactive to blood pressure variation than the arteries (which contain more [HbO]), but Δ[Hb] demonstrated the least magnitude and SNR in the LFOs. Therefore, we excluded the Δ[Hb] from the following discussion. A flowchart of LFO extraction and processing, and data analysis methods, is shown in Fig. 2.

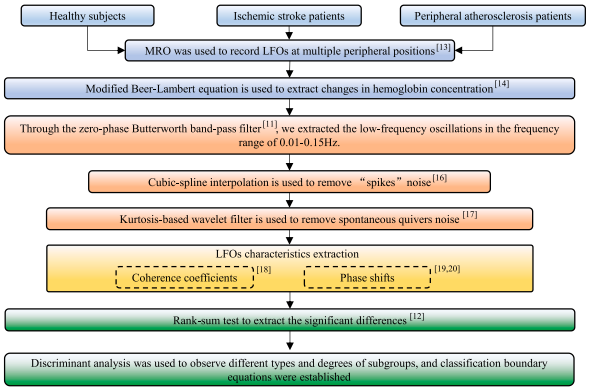

Fig. 2. LFO extraction, processing and analysis methodology.

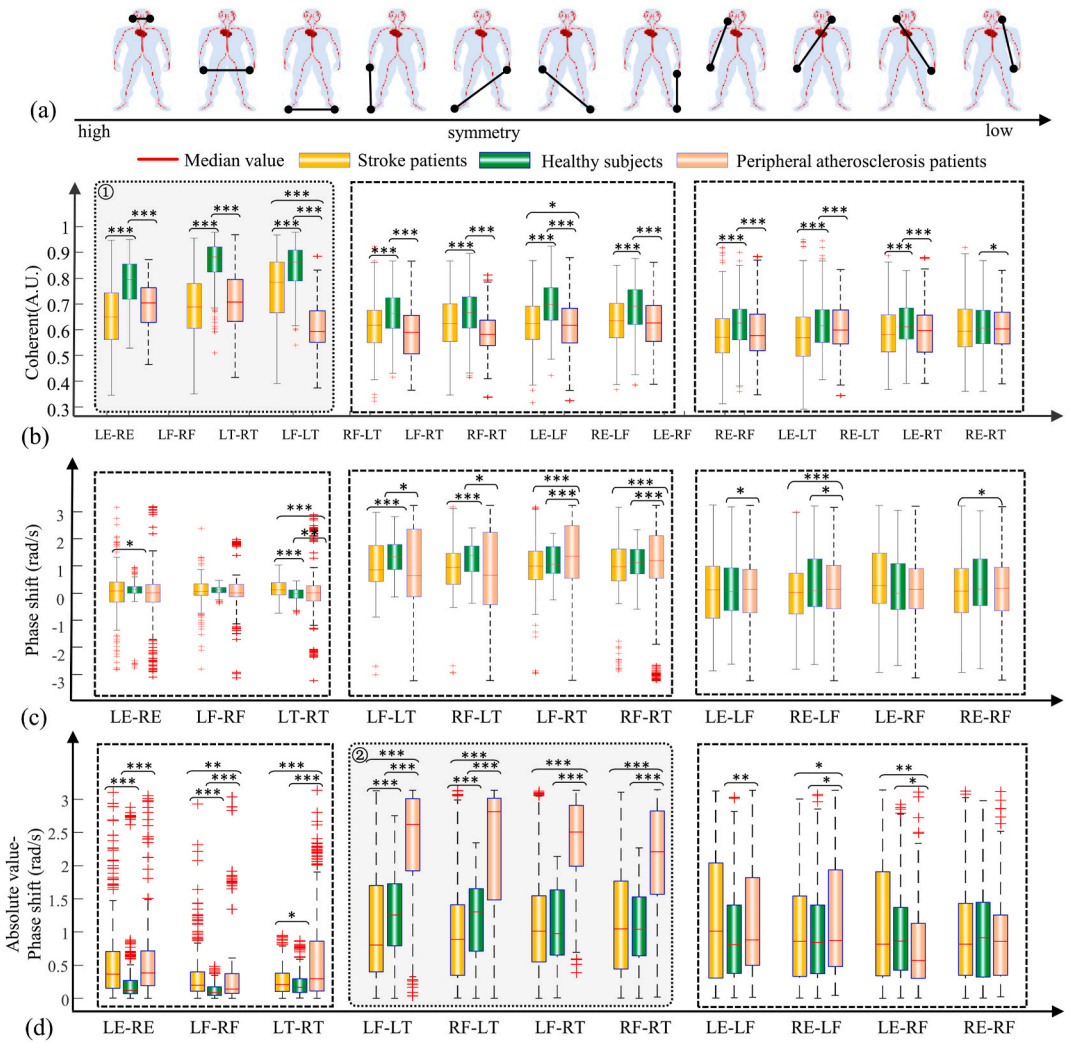

Fig. 3. The peripheral positions corresponding to different LFOs characteristics (a). The significant differences for (b) coherence coefficients, (c) phase shifts and (d) absolute value-phase shift variance among healthy controls, ischemic stroke patients and peripheral atherosclerosis patients, showing peripheral sources in symmetric and asymmetric positions for a paired-sample rank-sum test. $p < 0.001$(***), $p < 0.01$(**), $p < 0.05$(*).

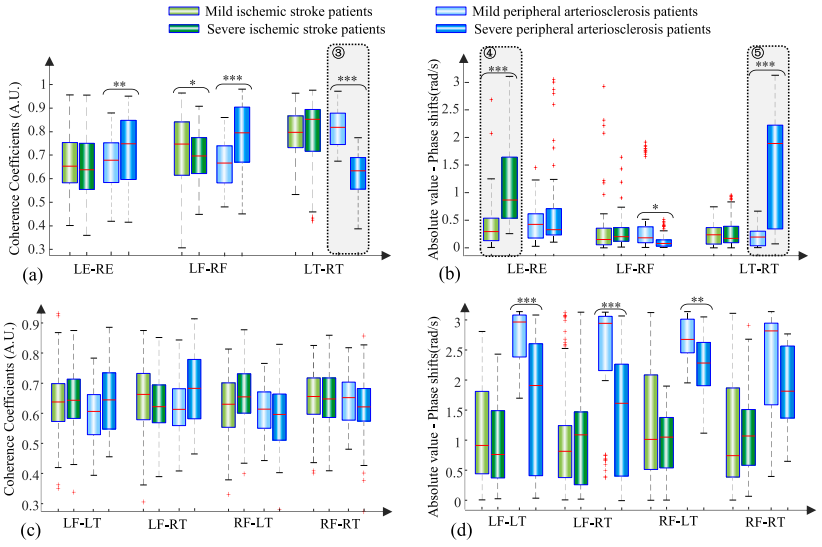

Fig. 4. Correlation coefficients (a) and absolute value-phase shifts (b) of the symmetric peripheral positions in mild and severe patients. Correlation coefficients (c) and absolute value-phase shifts (d) of finger and toe positions in mild and severe patients. $p < 0.001$(***), $p < 0.01$(**), $p < 0.05$(*).

3. Results

3.1. The characteristic differences in LFOs among patients of different types

We analyzed the coherence coefficients, phase shifts and absolute value-phase shifts of the LFOs from 64 volunteers of three types—25 healthy controls, 25 ischemic stroke patients and 14 peripheral atherosclerosis patients, as shown in Fig. 3. The peripheral positions corresponding to different LFOs characteristics are shown in Fig. 3 (a).

The results showed that the correlation coefficients for the symmetric and asymmetric peripheral positions were higher in healthy controls than in ischemic stroke patients and peripheral atherosclerosis patients. It should be noted that there was little overlap between the distribution of symmetrical peripheral coherence coefficients between healthy controls and the two types of patients (ischemic stroke and peripheral atherosclerosis patients, marked ①). The mean and standard deviation of the coherence coefficients in the symmetrical positions were 0.8 ± 0.09, 0.87 ± 0.08 and 0.85 ± 0.08 in the healthy subjects, while they were 0.66 ± 0.13, 0.7 ± 0.12 and 0.77 ± 0.13 in the ischemic stroke patients, and 0.69 ± 0.12, 0.71 ± 0.10, 0.70 ± 0.11 in the peripheral atherosclerosis patients. There were significant differences in the symmetric peripheral positions' coherence coefficients ($p < 0.001$) between healthy controls and ischemic stroke patients and peripheral atherosclerosis patients, as shown in Fig. 3 (b).

In Fig. 3 (c), the phase shifts between fingers and toes (including LF-LT, RF-LT, RF-LT, RF-RT) in the peripheral arteriosclerosis patients were significantly different from those in the ischemic stroke patients and healthy controls. However, there was considerable overlap in the phase shift distribution. Therefore, we conducted additional analyses of the absolute value-phase shifts, as shown in Fig. 3 (d). The results showed that the absolute value-phase shifts between the fingers and the toes in the peripheral arteriosclerosis patients were significantly greater than those in the healthy controls ($p < 0.001$) and the ischemic stroke patients ($p < 0.001$). There was little overlap in absolute value-phase shift distribution between peripheral arteriosclerosis patients and other subgroups (Marked ②). This may have been due to emboli in the lower extremities of peripheral arteriosclerosis patients increasing the spectral difference between the blood flow to the fingers and toes. The mean and standard deviation of absolute value-phase shifts between fingers and toes were 1.23 ± 0.61, 1.21 ± 0.60, 1.07 ± 0.57 and 1.06 ± 0.56 in the healthy subjects, while they were 1.06 ± 0.80, 1.0 ± 0.80, 1.17 ± 0.82 and 1.17 ± 0.81 in the ischemic stroke patients, and 2.27 ± 0.91, 2.16 ± 1.03, 2.31 ± 0.69 and 2.01 ± 0.86 in the peripheral atherosclerosis patients, as shown in Fig. 3 (d).

3.2. The characteristic differences in the LFOs in patients of different degrees

We further explored the differences of LFO characteristics between different degrees in ischemic stroke patients and peripheral arteriosclerosis patients, as shown in Fig. 4. The results showed that there were significant differences in LF-RF coherence coefficients ($p < 0.05$) and LE-RE absolute value-phase shifts ($p < 0.001$) between mild and severe ischemic stroke patients. Among them, the difference in LE-RE absolute value-phase shifts was greater (Marked ④). There were significant differences in symmetric peripheral coherence coefficients (LE-RE: $p < 0.01$, LF-RF: $p < 0.001$, LT-RT: $p < 0.001$) and asymmetric finger and toe absolute value-phase shifts (LF-RF: $p < 0.05$, LT-RT: $p < 0.001$) between mild and severe peripheral arteriosclerosis patients. The results showed that there was little overlap between mild and severe peripheral arteriosclerosis patients in LT-RT coherence coefficients (Marked ③) and LT-RT absolute value-phase shifts (Marked ⑤), as shown in Fig. 4 (a) and (b). Although there were significant differences in the absolute

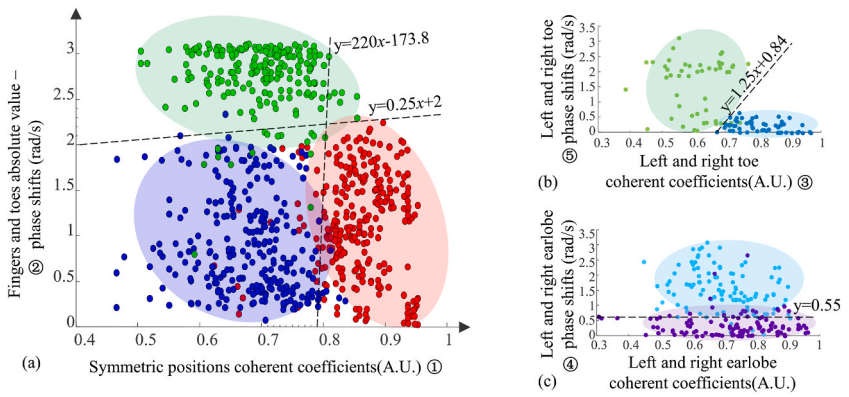

Fig. 5. Discriminant analysis was used to classify the observed data and further establish classification boundaries for types (a) and degrees (b)(c) of patient characteristic data.

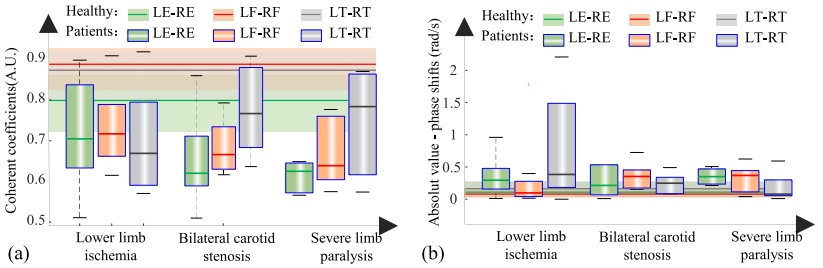

Fig. 6. Coherence coefficients (a) and phase shifts (b) for LFOs in patients with different circulatory disorders.

value-phase shifts of the fingers and the toes (LF-LT: $p < 0.001$, LF-RT: $p < 0.001$, RF-LT: $p < 0.01$) between mild and severe in peripheral arteriosclerosis patients, there was considerable overlap in data distribution. Thus, the coherence coefficients or phase shifts in fingers and toes are not suitable for distinguishing degrees or types, as shown in Fig. 4 (c) and (d).

3.3. *Classifying observations using discriminant analysis*

We used discriminant analysis to categorize three types and two degrees of subgroups, to further validate LFOs' effectiveness in differentiating between types and degrees of vascular injury disease. Based on the analysis results in Figs. 3 and 4, we used the coherence coefficients of symmetric positions (Marked ① in Fig. 3 (b)) and absolute value-phase shifts of fingers and toes (Marked ② in Fig. 3 (d)) as input to distinguish subgroup types; the coherence coefficients of LT-RT (marked ③ in Fig. 4 (a)) and absolute value-phase shifts of LT-RT (Marked ⑤ in Fig. 4 (b)) were used to distinguish the degrees of peripheral atherosclerosis subgroups; the absolute value-phase shifts of LE-RE (Marked ④in Fig. 4 (b)) were used to distinguish the degrees of ischemic stroke patients. Finally, we identified the classification boundary equations (classify.m in MATLAB) between different subgroup types and degrees, as shown in Fig. 5.

The results showed that the classification boundary between the healthy controls and the clinical patients was $y = 0.25\,x + 2$, and between the ischemic stroke patients and the peripheral atherosclerosis patients it was $y = 220\,x - 173.8$, as shown in Fig. 5 (a). The classification boundary between the peripheral atherosclerosis patients with different degrees was $y = 1.25\,x + 0.84$, and between the ischemic stroke patients with different degrees, it was $y = 0.55$, as shown in Fig. 5 (b) and (c). The accuracy of differentiating between types of patients was 70%; those with different degrees of peripheral atherosclerosis was 85%, and those with different degrees of ischemic stroke was 72%. These results demonstrated that LFOs can be used to identify the types and degrees of vascular injuries.

4. Discussion

4.1. *Differences in lower limb arteries, carotid arteries and severe paralysis patients*

We screened out 5 patients with lower limb ischemia (weakened lower limb skin elasticity, dark, or even broken skin), 4 patients with bilateral carotid artery stenosis (dizziness, loss of memory, slurred speech), and 4 patients with severe paralysis from all subjects, and discussed the transmission characteristics of LFOs in patients with different symptoms, as shown in Fig. 6. The results showed that the LE-RE coherence coefficients were lower in carotid artery stenosis and severe paralysis patients than in lower limb ischemia

patients, with the lowest in severe paralysis patients. The LT-RT phase shifts were significantly greater in lower limb ischemia patients, while the LE-RE phase shifts were greater in carotid artery and severe paralysis patients. These findings indicated that different vascular stenosis locations have different effects on local blood flow. When the blood exits the heart at the ascending aorta, there are divergent pathways for blood traveling to different locations in the body. When lesions or narrowing occur on different vascular pathways, the blood travels to its specific destination in the earlobes, fingers and toes, or the draining veins of the brain. The frequencies and amplitudes of the signals it carries may be affected differentially by physiological effects resulting from regional circulatory changes, as well as local oxygen demands and vasodilation [10]. Therefore, these effects can account for variations between the LFO signals recorded at the different sites.

4.2. The interaction between neurotic and nonneurotic LFOs

Several studies have demonstrated the neuronal component in the global Blood Oxygen Level Dependent (BOLD) signal [24,25]. We believe that both neurotic and nonneurotic LFOs contribute to the changes in hemodynamic parameter data, and this has been demonstrated in many multimodal [26,27] and invasive studies [28]. Mayer waves (~0.1 Hz) are systemic changes in arterial pressure, and they also are thought to contribute to LFOs, although the origin and purpose of these fluctuations is still debated [29]. Studies have associated LFOs measured in the head using NIRS with arterial pressure signals. Spectral coherence between mean arterial pressure and oxy-hemoglobin concentration change (Δ[HbO]) in the low-frequency range has been found to be useful in studying global (and regional) autoregulation [30]. The phase angle between arterial blood pressure and Δ[HbO] or deoxy-hemoglobin concentration change (Δ[Hb]) around 0.1 Hz has been shown to be sensitive to carbon dioxide levels [31].

The above studies show that there is a close interaction between neurotic and non-neurotic LFOs. In this paper, we used the non-neurogenic components of these LFOs to track abnormal blood circulation. However, we do not deny neurogenic LFOs' contribution to the overall blood circulation. Since LFOs include both neuropathic and non-neuropathic components, we believe that LFOs have the potential to be used not only to assess diseases of clinical vascular injury, but also to be used to explore both central and peripheral interactions.

4.3. Application prospects of LFOs in the detection of vascular injury diseases

Many reports have indicated an association between comorbidities such as diabetes mellitus, history of heart failure, coronary heart disease, and atrial fibrillation or risk factors (smoking history) and stroke and peripheral arterial disease, or some combination of these outcomes [32]. Although the mechanism has not been elucidated, these factors undoubtedly affect neurological and/or hemodynamic changes. Thus, these factors are commonly used to assess ischemic stroke patients or peripheral arterial disease. However, this assessment method may lead to evaluation errors, such as patient description errors or clinical experience issues. Although some researchers have investigated neurological disorders, cerebrovascular diseases or peripheral arterial disease by examining electroencephalograph signals [33–35], this method remains challenging.

The results of our study showed that LFOs can distinguish patients with different types and degrees of vascular injury diseases, indicating that LFOs can be serve as perfusion biomarkers with the potential to influence the field of peripheral arteriosclerosis rehabilitation. Therefore, LFOs serve as natural tracking tools for abnormal changes in blood circulation, providing valuable information about patients that can assist researchers and clinicians in identifying specific biological subgroups. The development of peripheral LFOs for peripheral arterial disease research offers the following advantages. Firstly, LFOs are slow and spontaneous hemodynamic variations that can be treated as natural "tags" on the blood flow. Therefore, they are suitable for studying circulatory injury diseases. Peripheral LFOs may not be utilized directly to reflect the physiological state of the brain. The function of these LFOs is to reflect systemic physiological circulatory effects. Secondly, single tissue structures in peripheral positions lead to signal-to-noise that is superior to that of functional brain studies in which light must penetrate multiple layers of scattering media (i.e., the skin and skull) before reaching the cortex. Lastly, LFOs based on changes in oxygenation levels are available through Near Infrared Spectroscopy devices, which are typically portable, and simple to use. This will aid in future clinical applications.

4.4. Limitations of the study

In this study, there were 64 patients with small patient data sets. Further studies should expand this data set of subjects and further optimize the classification boundaries in this study using large samples to improve LFOs' accuracy in differentiating patients with different types and degrees of vascular injury. In addition, we will continue to expand the patients types and explore the ability to use LFOs to distinguish more vascular injury diseases.

5. Conclusion

Our study demonstrated that LFOs' transmission characteristics reflect the changes in the physiological processes, which can be used to reflect the abnormal blood circulation changes in patients with different types and degrees of vascular injury diseases. Combined with their portability and accessibility, LFOs may offer clinicians an additional tool to incorporate into their practice to improve patient prognostication, treatment allocation, and assessment of therapeutic response. In addition, studying these signals could provide baseline references for exploring the overall feedback of pericentral interactions.

Table 1
Mean, standard deviation, interquartile and median values of LFOs' characteristics in healthy subjects.

Positions		LE-RE	LF-RF	LT-RT	LF-LT	RF-LT	LF-RT	RF-RT	LE-LF	RE-LF	LE-RF	RE-RF
Coherence coefficients (A. U.)	mean	0.8	0.87	0.85	0.67	0.67	0.71	0.69	0.63	0.62	0.63	0.62
	standard deviation	0.09	0.08	0.08	0.09	0.1	0.09	0.1	0.09	0.1	0.08	0.09
	upper quartile	0.54	0.54	0.56	0.43	0.43	0.45	0.32	0.37	0.42	0.4	0.37
	lower quartile	0.57	0.6	0.61	0.46	0.43	0.5	0.4	0.39	0.42	0.41	0.39
	median	0.56	0.59	0.6	0.44	0.43	0.49	0.39	0.38	0.42	0.41	0.37
Phase Shifts (rad/s)	mean	−0.02	0.01	−0.15	1.22	1.19	1.05	1.03	−0.12	0	−0.07	0.1
	standard deviation	0.61	0.15	0.24	0.63	0.64	0.62	0.62	1.16	1.25	1.18	1.22
	upper quartile	−2.86	−0.48	−0.87	−0.23	−0.46	−0.33	−0.68	−2.79	−2.84	−2.86	−2.93
	lower quartile	−2.78	−0.44	−0.84	−0.18	−0.32	−0.28	−0.49	−2.64	−2.77	−2.78	−2.61
	median	−2.81	−0.46	−0.86	−0.22	−0.43	−0.3	−0.67	−2.7	−2.78	−2.8	−2.75
Absolute value-Phase Shifts (rad/s)	mean	0.29	0.12	0.22	1.23	1.21	1.07	1.06	0.94	0.99	0.97	0.98
	standard deviation	0.53	0.1	0.18	0.61	0.6	0.57	0.56	0.68	0.76	0.68	0.73
	upper quartile	0.27	0.18	0.3	1.73	1.65	1.64	1.53	1.41	1.41	1.37	1.45
	lower quartile	0.07	0.05	0.09	0.79	0.72	0.65	0.64	0.38	0.37	0.43	0.32
	median	0.12	0.09	0.17	1.26	1.31	0.98	1.04	0.81	0.84	0.86	0.91

Table 2
Mean, standard deviation, interquartile and median of LFOs' characteristics in ischemic stroke patients.

		LE-RE	LF-RF	LT-RT	LF-LT	RF-LT	LF-RT	RF-RT	LE-LF	RE-LF	LE-RF	RE-RF
Coherence coefficients (A. U.)	mean	0.66	0.7	0.77	0.63	0.64	0.63	0.64	0.59	0.59	0.6	0.61
	standard deviation	0.13	0.12	0.13	0.1	0.1	0.09	0.09	0.11	0.12	0.1	0.11
	upper quartile	0.36	0.31	0.41	0.34	0.32	0.34	0.38	0.28	0.31	0.38	0.37
	lower quartile	0.37	0.34	0.42	0.36	0.36	0.39	0.41	0.34	0.31	0.39	0.39
	median	0.37	0.31	0.42	0.35	0.36	0.37	0.4	0.32	0.31	0.39	0.38
Phase Shifts (rad/s)	mean	−0.08	−0.03	0.07	0.94	0.87	0.89	0.84	−0.02	−0.15	0.11	−0.01
	standard deviation	0.87	0.52	0.34	0.94	0.95	1.12	1.15	1.55	1.29	1.44	1.21
	upper quartile	−2.94	−2.79	−0.83	−3.07	−3.07	−3.09	−3	−3.06	−2.98	−3.13	−3.1
	lower quartile	−2.91	−2.14	−0.8	−1.8	−3.06	−3.08	−2.93	−2.95	−2.89	−3.1	−3.01
	median	−2.93	−2.3	−0.81	−2.87	−3.07	−3.09	−2.96	−2.99	−2.91	−3.1	−3.03
Absolute value-Phase Shifts (rad/s)	mean	0.59	0.33	0.27	1.06	1.01	1.17	1.17	1.21	1.03	1.14	0.96
	standard deviation	0.65	0.39	0.22	0.8	0.8	0.82	0.81	0.96	0.8	0.89	0.74
	upper quartile	0.71	0.4	0.38	1.7	1.41	1.55	1.77	2.04	1.54	1.91	1.43
	lower quartile	0.16	0.11	0.1	0.4	0.35	0.55	0.44	0.31	0.34	0.34	0.35
	median	0.37	0.2	0.21	0.81	0.89	1.01	1.05	1.01	0.86	0.82	0.82

Author contributions

Yunfei Ma contributed reagents, materials, analysis tools or data and wrote the paper; Kexin Luo and Peng Ding analyzed and interpreted the data; Shimin Yin performed the experiments; Xiaoli Li and Yingwei Li conceived and designed the experiments.

Funding

This research was financially supported by the National Natural Science Foundation of China (Grant No. 61827811), the Hebei Province Funding Project for the Introduction of Overseas Students (Grant No. C20200364) and the Natural Science Foundation of Hubei Province (Grant No. 2022CFB524). We gratefully acknowledge all editors and anonymous reviewers.

Institutional review board statement

This study was conducted in accordance with the Declaration of Helsinki, and approved by the ethics committee at PLA Rocket Force Characteristic Medical Center and McLean Hospital (KY2021036).

Table 3
Mean, standard deviation, interquartile and median of LFOs' characteristics in peripheral atherosclerosis patients.

		LE-RE	LF-RF	LT-RT	LF-LT	RF-LT	LF-RT	RF-RT	LE-LF	RE-LF	LE-RF	RE-RF
Coherence coefficients (A. U.)	mean	0.69	0.71	0.70	0.61	0.63	0.61	0.62	0.59	0.59	0.60	0.60
	standard deviation	0.12	0.10	0.11	0.07	0.08	0.04	0.06	0.08	0.08	0.08	0.09
	upper quartile	0.51	0.58	0.57	0.52	0.50	0.50	0.51	0.50	0.50	0.51	0.49
	lower quartile	0.52	0.58	0.57	0.52	0.53	0.50	0.52	0.52	0.50	0.51	0.49
	median	0.51	0.58	0.57	0.52	0.53	0.50	0.52	0.52	0.50	0.51	0.49
Phase Shifts (rad/s)	mean	−0.05	0.06	−0.06	0.36	0.34	1.39	1.01	0.17	0.29	0.25	0.35
	standard deviation	0.43	0.54	0.99	1.42	1.60	1.61	1.47	0.98	0.78	0.72	0.77
	upper quartile	−0.96	−0.63	−2.14	−2.12	−1.93	−2.97	−2.87	−2.10	−1.08	−0.83	−1.15
	lower quartile	−0.95	−0.63	−2.14	−2.12	−1.92	−2.97	−2.87	−2.10	−1.08	−0.83	−1.15
	median	−0.96	−0.63	−2.14	−2.12	−1.92	−2.97	−2.87	−2.10	−1.08	−0.83	−1.15
Absolute value-Phase Shifts (rad/s)	mean	0.66	0.36	0.730	2.27	2.16	2.31	2.02	1.12	1.21	0.85	0.94
	standard deviation	0.73	0.57	0.81	0.92	1.03	0.7	0.86	0.75	0.92	0.69	0.64
	upper quartile	0.72	0.37	1.1	3	3.01	2.86	2.8	1.83	1.94	1.26	1.28
	lower quartile	0.19	0.07	0.16	1.86	1.48	1.98	1.54	0.5	0.48	0.33	0.45
	median	0.41	0.13	0.33	2.59	2.79	2.49	2.14	0.88	0.88	0.6	0.88

Table 4
p-values before and after correction for multiple comparisons about healthy subjects and stroke patients.

	Coherent		Phase Shift		Absolute value-Phase Shift	
Positions	*p*-value	Adjusted *p* -valuE	*p* -value	Adjusted *p* -valuE	*p* -value	Adjusted *p* -valuE
LE-RE	2.54e-34	1.90e-33	0.026	0.065	4.22e-18	8.28e-17
LF-RF	4.81e-51	7.22e-50	0.175	0.219	8.28e-17	4.22e-18
LT-RT	5.93e-14	2.22e-13	4.99e-13	7.49e-12	9.69e-06	0.03
LF-LT	8.67e-09	1.62e-08	1.34e-05	6.69e-05	0.0007	0.0007
RF-LT	6.25e-05	8.52e-05	1.04e-07	7.81e-07	0.03	9.69e-06
LF-RT	8.86e-18	4.43e-17	0.056	0.093	0.039	0.97
RF-RT	3.13e-11	6.70e-11	0.084	0.125	0.32	0.76
LE-LF	1.04e-07	1.73e-07	0.658	0.658	0.76	0.03
RE-LF	2.15e-06	3.23e-06	0.132	0.179	0.81	0.82
LE-RF	0.0001	0.0002	0.0261	0.065	0.97	0.32
RE-RF	0.49	0.485	0.179	0.219	0.97	0.97

Table 5
p-values before and after correction for multiple comparisons about healthy subjects and peripheral atherosclerosis patients.

	Coherent		Phase Shift		Absolute value-Phase Shift	
Positions	*p* -value	Adjusted *p* -valuE	*p* -value	Adjusted *p* -valuE	*p* -value	Adjusted *p* -valuE
LE-RE	3.98e-13	1.49e-12	0.03	0.05	3.33e-42	5.77e-17
LF-RF	1.99e-32	2.99e-31	0.0.6	0.07	6.04e-29	4.37e-06
LT-RT	1.34e-30	1.05e-29	0.007	0.007	6.68e-26	2.35e-10
LF-LT	2.40e-10	6.01e-10	0.039	0.40	1.29e-20	6.04e-29
RF-LT	1.25e-05	1.87e-05	0.034	0.04	5.77e-17	1.29e-20
LF-RT	3.81e-23	1.90e-22	4.93e-16	7.39e-15	2.35e-10	3.33e-42
RF-RT	3.41e-12	1.02e-11	2.51e-6	9.42e-6	4.37e-06	6.68e-26
LE-LF	0.00093	0.00099	0.01	0.02	0.03	0.03
RE-LF	0.00058	0.00067	0.02	0.04	0.03	0.05
LE-RF	0.00048	0.00061	9e-3	0.02	0.05	0.03
RE-RF	0.026	0.02637	0.03	0.05	0.86	0.86

Informed consent statement

The code generated and analyzed in this study is available from the corresponding author upon reasonable request.

Data availability statement

The datasets generated and analyzed in this study are available from the corresponding author upon reasonable request.

Table 6
p-values before and after correction for multiple comparisons about stroke patients and peripheral atherosclerosis patients.

	Coherent		Phase Shift		Absolute value-Phase Shift	
Positions	*p* -value	Adjusted *p* -valuE	*p* -value	Adjusted *p* -valuE	*p* -value	Adjusted *p* -valuE
LE-RE	0.03	0.11	0.78	0.81	1.89e-29	0.38
LF-RF	0.80	0.80	0.63	0.79	1.96e-28	0.024
LT-RT	1.31e-19	1.97e-08	1.27e-4	4.41e-4	7.95e-24	1.62e-06
LF-LT	0.03	0.11	0.70	0.80	6.75e-19	1.96e-28
RF-LT	0.14	0.27	0.22	0.29	1.62e-06	7.95e-24
LF-RT	3.27e-4	0.0025	3.16e-6	4.75e-5	0.014	1.89e-29
RF-RT	0.04	0.11	7.51e-6	4.23e-5	0.02	6.75e-19
LE-LF	0.15	0.27	0.05	0.10	0.07	0.98
RE-LF	0.46	0.53	1.38e-4	4.40e-4	0.38	0.077
LE-RF	0.56	0.60	0.73	0.81	0.97	0.014
RE-RF	0.15	0.27	4.69e-4	0.001	0.98	0.97

Declaration of competing interest

The authors declare that they have no known competing financial interests or personal relationships that could have appeared to influence the work reported in this paper.

Acknowledgements

We would like to thank the editor and reviewers for their comments, which will improve the manuscript significantly.

Appendix A

The median, mean, and standard deviation of LFOs' characteristics were calculated for all healthy individuals, ischemic stroke patients and peripheral arteriosclerosis patients, as shown in Tables 1–3. We improved the judgment standard (*p*-value) to reduce the positive results' error rates (FDR value). Then, we used the Benjamini-Hochberg method to correct the results. *p*-values before and after correction are shown in Tables 4–6; the correction can maintain a false-positive probability below 0.05.

References

[1] H. Yang, B. Inglis, T.M. Talavage, et al., Coupling between cerebrovascular oscillations and CSF flow fluctuations during wakefulness: an fMRI study, J. Cerebr. Blood Flow Metabol. 42 (6) (2022) 1091–1103.
[2] A. Sassaroli, M. Pierro, P.R. Bergethon, et al., Low-frequency spontaneous oscillations of cerebral hemodynamics investigated with near-infrared spectroscopy: a Review, IEEE J. Sel. Top Quant. 18 (4) (2012) 1478–1492.
[3] Y. Tong, K.P. Lindsey, L.M. Hocke, et al., Perfusion information extracted from resting state functional magnetic resonance imaging, J. Cerebr. Blood Flow Metabol. 37 (2) (2017) 564–576.
[4] L.N. Livera, Y.A. Wickramasinghe, S.A. Spencer, et al., Cyclical fluctuations in cerebral blood volume, Arch. Dis. Child. 67 (1) (1992) 62–63.
[5] Y. Hoshi, S. Kosaka, Y. Xie, et al., Relationship between fluctuations in the cerebral hemoglobin oxygenation state and neuronal activity under resting conditions in man, Neurosci. Lett. 245 (3) (1998) 147–150.
[6] H. Obrig, M. Neufang, R. Wenzel, et al., Spontaneous low frequency oscillations of cerebral hemodynamics and metabolism in human adults, Neuroimage 12 (6) (2000) 623–639.
[7] Z. Li, M. Zhang, Q. Xin, et al., Correlation analysis between prefrontal oxygenation oscillations and cerebral artery hemodynamics in humans, Microvasc. Res. 82 (3) (2011) 304–310.
[8] X.N. Zuo, A.D. Martino, C. Kelly, et al., The oscillating brain: complex and reliable, Neuroimage 49 (2) (2010) 1432–1445.
[9] Y. Tong, L.M. Hocke, L.D. Nickerson, et al., Evaluating the effects of systemic low frequency oscillations measured in the periphery on the independent component analysis results of resting state networks, Neuroimage 76 (1) (2013) 202–215.
[10] Y. Tong, L.M. Hocke, S.C. Licata, et al., Low-frequency oscillations measured in the periphery with near-infrared spectroscopy are strongly correlated with blood oxygen level-dependent functional magnetic resonance imaging signals, J. Biomed. Opt. 17 (10) (2012), 106004.
[11] Y. Li, H. Zhang, M. Yu, et al., Systemic low-frequency oscillations observed in the periphery of healthy human subjects, J. Biomed. Opt. 23 (5) (2018) 1–11.
[12] Y. Li, Y. Ma, S. Ma, et al., Asymmetry of peripheral vascular biomarkers in ischemic stroke patients, assessed using NIRS, J. Biomed. Opt. 25 (6) (2020) 1–16.
[13] Y. Li, Y. Ma, S. Ma, et al., A low-cost multichannel NIRS oximeter for monitoring systemic low-frequency oscillations, Neural Comput. Appl. 32 (10) (2020) 15629–15641.
[14] R.W. Paynter, Modification of the Beer-Lambert equation for application to concentration gradients, Surf. Interface Anal. 3 (4) (1997) 186–187.
[15] L.M. Hocke, Y. Tong, K.P. Lindsey, et al., Comparison of peripheral near-infrared spectroscopy low-frequency oscillations to other denoising methods in resting state functional MRI with ultrahigh temporal resolution, Magn. Reson. Med. 76 (6) (2016) 1697–1707.
[16] S.A. Dyer, J.S. Dyer, Cubic-spline interpolation.1, IEEE Instrum. Meas. Mag. 4 (1) (2001) 44–46.
[17] A.M. Chiarelli, E.L. Maclin, M. Fabiani, et al., A kurtosis-based wavelet algorithm for motion artifact correction of fNIRS data, Neuroimage 112 (2015) 128–137.
[18] Z. Xin, J. Yu, R. Zhao, et al., Activation detection in fNIRS by wavelet coherence, J. Biomed. Opt. 20 (1) (2015), 016004.
[19] Y. Bai, X. Xia, Y. Wang, et al., Fronto-parietal coherence response to tDCS modulation in patients with disorders of consciousness, Int. J. Neurosci. 128 (7) (2018) 587–594.
[20] M.L. Pierro, A. Sassaroli, P.R. Bergethon, et al., Phase-amplitude investigation of spontaneous low-frequency oscillations of cerebral hemodynamics with near-infrared spectroscopy: a sleep study in human subjects, Neuroimage 63 (3) (2012) 1571–1584.

[21] G. Taga, H. Watanabe, F. Homae, Spatial variation in the hemoglobin phase of oxygenation and deoxygenation in the developing cortex of infants, Neurophotonics 5 (1) (2018), 011017.
[22] H. Niu, S. Khadka, F. Tian, et al., Resting-state functional connectivity assessed with two diffuse optical tomographic systems, J. Biomed. Opt. 16 (4) (2011), 046006.
[23] Y.J. Zhang, C.M. Lu, B.B. Biswal, et al., Detecting resting-state functional connectivity in the language system using functional near-infrared spectroscopy, J. Biomed. Opt. 15 (4) (2010), 047003.
[24] X. Liu, T. Yanagawa, D.A. Leopold, et al., Robust longrange coordination of spontaneous neural activity in waking, sleep and anesthesia, Cerebr. Cortex 25 (9) (2015) 2929–2938.
[25] M.L. Scholvinck, A. Maier, F.Q. Ye, et al., Neural basis of global resting-state fMRI activity, Proc. Natl. Acad. Sci. U S A. 107 (22) (2010) 10238–10243.
[26] E. Martinez-Montes, P.A. Valdes-Sosa, F. Miwakeichi, et al., Concurrent EEG/fMRI analysis by multiway partial least squares, Neuroimage 22 (3) (2004) 1023–1034.
[27] T. Hiltunen, J. Kantola, A. Abou Elseoud, et al., Infra-slow EEG fluctuations are correlated with resting-state network dynamics in fMRI, J. Neurosci. 34 (2) (2014) 356–362.
[28] X. Liu, T. Yanagawa, D.A. Leopold, et al., Robust longrange coordination of spontaneous neural activity in waking, sleep and anesthesia, Cerebr. Cortex 25 (9) (2015) 2929–2938.
[29] C. Julien, The enigma of Mayer waves: facts and models, Cardiovasc. Res. 70 (1) (2006) 12–21.
[30] M.D. Papademetriou, I. Tachtsidis, M.J. Elliot, et al., Multichannel near infrared spectroscopy indicates regional variations in cerebral autoregulation in infants supported on extracorporeal membrane oxygenation, J. Biomed. Opt. 17 (6) (2012), 067008.
[31] S.J. Payne, J. Mohammad, M.M. Tisdall, et al., Effects of arterial blood gas levels on cerebral blood flow and oxygen transport, Biomed. Opt Express 2 (4) (2011) 966–979.
[32] K. Masashi, M. Noguchi, H. Kubo, et al., Pre-stroke frailty and stroke severity in elderly patients with acute stroke, J. Stroke Cerebrovasc. 29 (12) (2020), 105346.
[33] H. Ke, D. Chen, T. Shah, et al., Cloud-aided online EEG classification system for brain healthcare: a case study of depression evaluation with a lightweight CNN, Software Pract. Ex. 50 (5) (2020) 596–610.
[34] K. Hengjin, D. Chen, B. Shi, et al., Improving brain e-health services via high-performance eeg classification with grouping bayesian optimization, IEEE T. Serv. Comput. 13 (4) (2020) 696–708.
[35] K. Hengjin, W. Fengqin, M. Hongying, et al., ADHD identification and its interpretation of functional connectivity using deep self-attention factorization, Knowl. - based syst. 250 (2022), 109082.